

Surface Radiation Processes in the Tropical Pacific

Catherine GAUTIER and Robert FROUIN

*California Space Institute, A-021
Scripps Institution of Oceanography
La Jolla, CA 92093 - U.S.A.*

This short article is a summary of the results contained in a forthcoming article (Gautier and Frouin, 1989) investigating net surface solar irradiance variability in the central and eastern tropical Pacific from GOES satellite data for the period 1982-1985. This period covers the 1982-1983 El Niño event during which major changes took place in the coupled atmosphere-ocean system. The satellite estimates provide an unprecedented and accurate description of the spatial and temporal variability of the surface solar radiation on a daily (to monthly) basis and a 50 km spatial scale.

The first result of the study was a preliminary assessment (see Fig. 1) of existing climatologies by comparing them with the mean annual satellite estimates (over the October 1983 to September 1985 period), which are expected to be accurate to better than 15 Wm^{-2} . In Fig. 1 the climatological val-

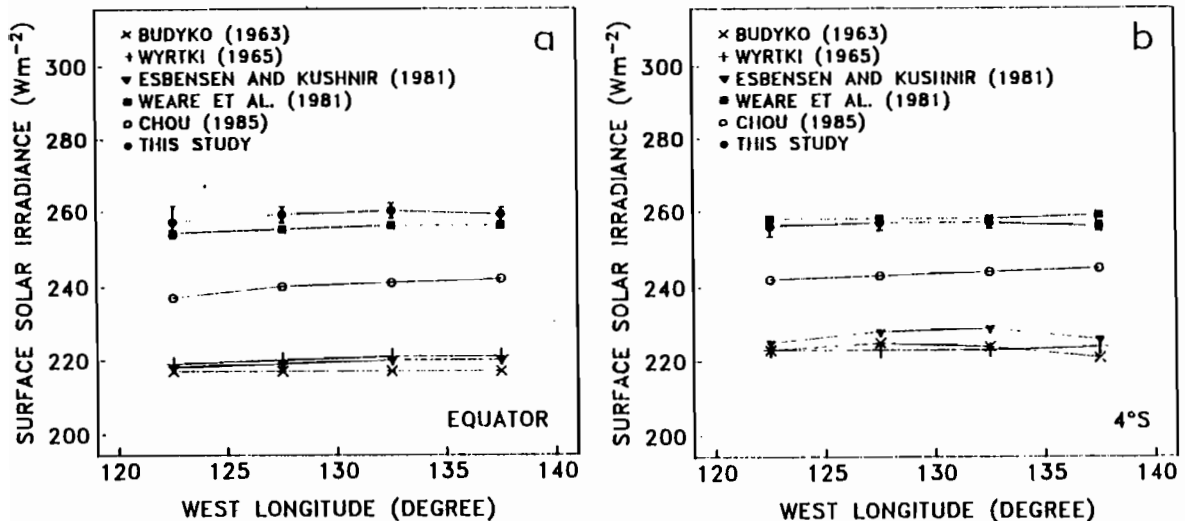


Fig. 1 Comparison of annually-averaged net surface solar irradiance obtained by various authors and computed with the satellite technique of Gautier et al. (1980) in regions centered at the equator (a) and at 4°S (b). Each point corresponds to $4^\circ \text{ lat. by } 5^\circ \text{ lon.}$ averages. The vertical bars (satellite technique only) represent the spatial standard deviation in the $4^\circ \text{ lat. by } 5^\circ \text{ lon.}$ areas.

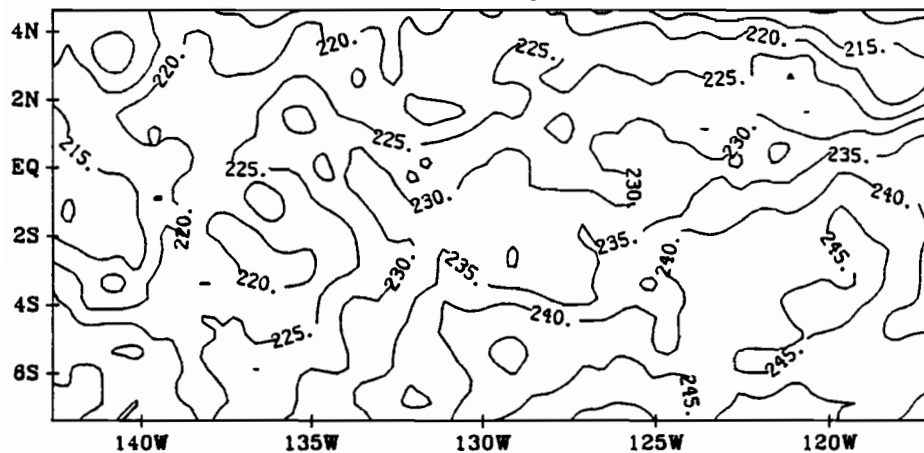
ues at the equator computed by Budyko (1963), Chou (1985), Esbensen and Kushnir (1981), and Wyrтки (1965) all appear to underestimate solar irradiance

at the surface by about 20 to 40 Wm^{-2} , whereas those computed by Weare et al. (1981) are very close (within 1 to 2 Wm^{-2}) to the satellite estimations. When the annual mean is computed by including the El Niño conditions, the satellite estimations are reduced by only 8 Wm^{-2} , suggesting that most climatologies underestimate solar irradiance at the surface.

The spatial variability of the annual net solar irradiance depicted from the satellite data is illustrated in Fig. 2a and b for the periods Oct. 1982 – Sept. 1983 and Oct. 1983 – Sept. 1984. Also included in Fig. 2a and b are the corresponding temporal standard deviation fields. During non-El Niño periods (Fig 2b), the annually averaged net solar irradiance field is dominated by very weak zonal gradients (1 to 2 Wm^{-2} over 2000 km) and stronger meridional ones (up to 20 Wm^{-2} over 200 km) in the region of the ITCZ. The standard deviation field also has weak zonal gradients and its maximum values (about 25 Wm^{-2}) are found in the southern part of the study area. During the El Niño period (Fig 2a), the zonal variability becomes as large as the meridional variability, particularly in the central Pacific, where intense convection dominates the atmospheric state. The standard deviation from the annual mean reaches 40 Wm^{-2} in that region, much larger than that observed within the ITCZ region during non-El Niño years. A difference of more than 150 Wm^{-2} in surface solar irradiance takes place in the equatorial region between 140° and 180° W between January 1981 and January 1983, where the largest SST anomaly is observed. The variability of the standard deviation reflects the large changes in surface solar irradiance occurring during the El Niño year. Its maximum values (about 45 Wm^{-2}) are found in the western part of the study area.

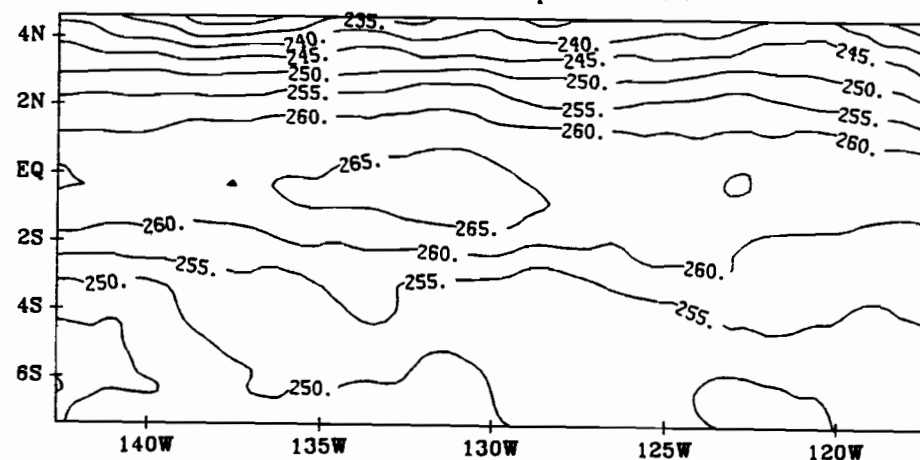
A general view of the seasonal and interannual variations of the net surface solar irradiance is obtained by condensing the data into diagrams of latitude (and longitude) versus time. Such diagrams, illustrated in Fig. 3a and b, have been obtained by averaging the data longitudinally (and meridionally) over the entire domain. The latitude versus time diagram (Fig. 3a) shows the meridional extension of low net surface solar irradiance values (less than 160 Wm^{-2}) covering the entire study area starting in November 1982 and retreating in May 1983. These low values are associated in the north with the ITCZ, but their large meridional extent suggests that they are also related to processes other than ITCZ displacements. The longitude versus time diagram (Fig. 3b) supports this statement and shows a large zonal extension of the low net surface solar irradiance values. This extension is associated with the eastward displacement of the main region of convection/precipitation, as mentioned above.

Annually-Averaged Net Surface Solar Irradiance (Wm^{-2})
(October 1982 – September 1983)



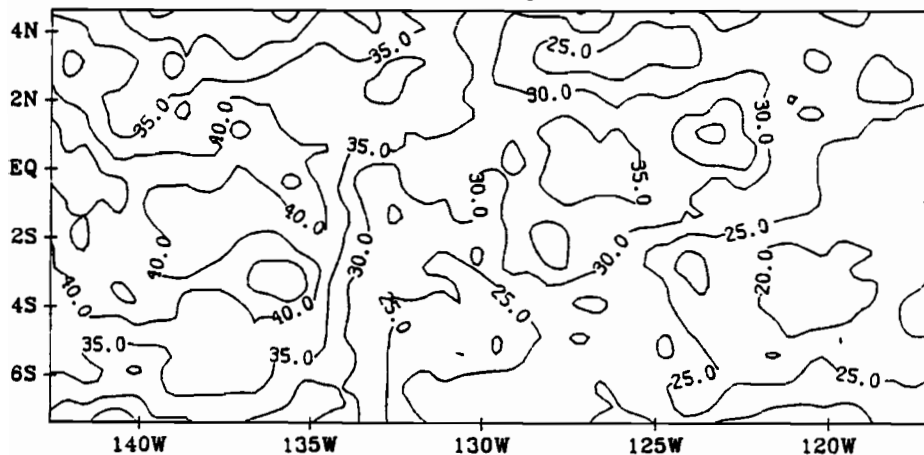
a

Annually-Averaged Net Surface Solar Irradiance (Wm^{-2})
(October 1983 – September 1984)



b

Standard Deviation (Wm^{-2})
(October 1982 – September 1983)



Standard Deviation (Wm^{-2})
(October 1983 – September 1984)

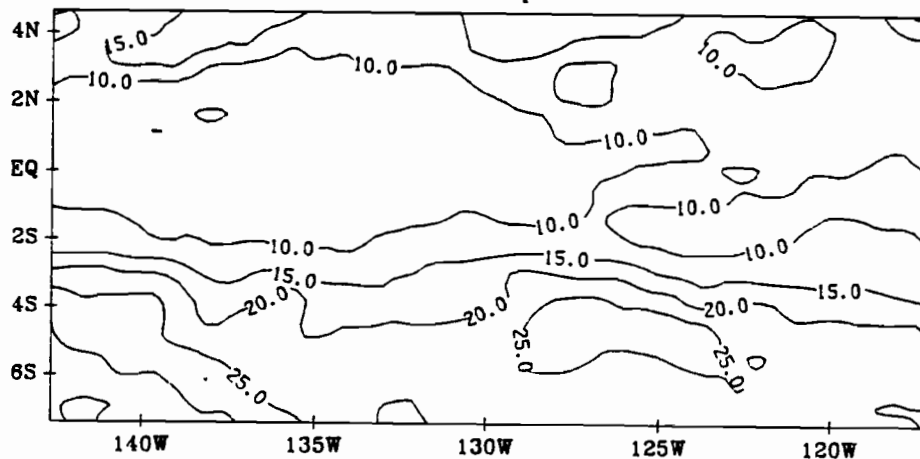


Fig. 2 Spatial distribution of annually-averaged net surface solar irradiance (computed with the satellite technique of Gautier et al., 1980) for the periods October 1982–September 1983 (a) and October 1983–September 1984 (b). The corresponding temporal standard deviation fields are also shown below.

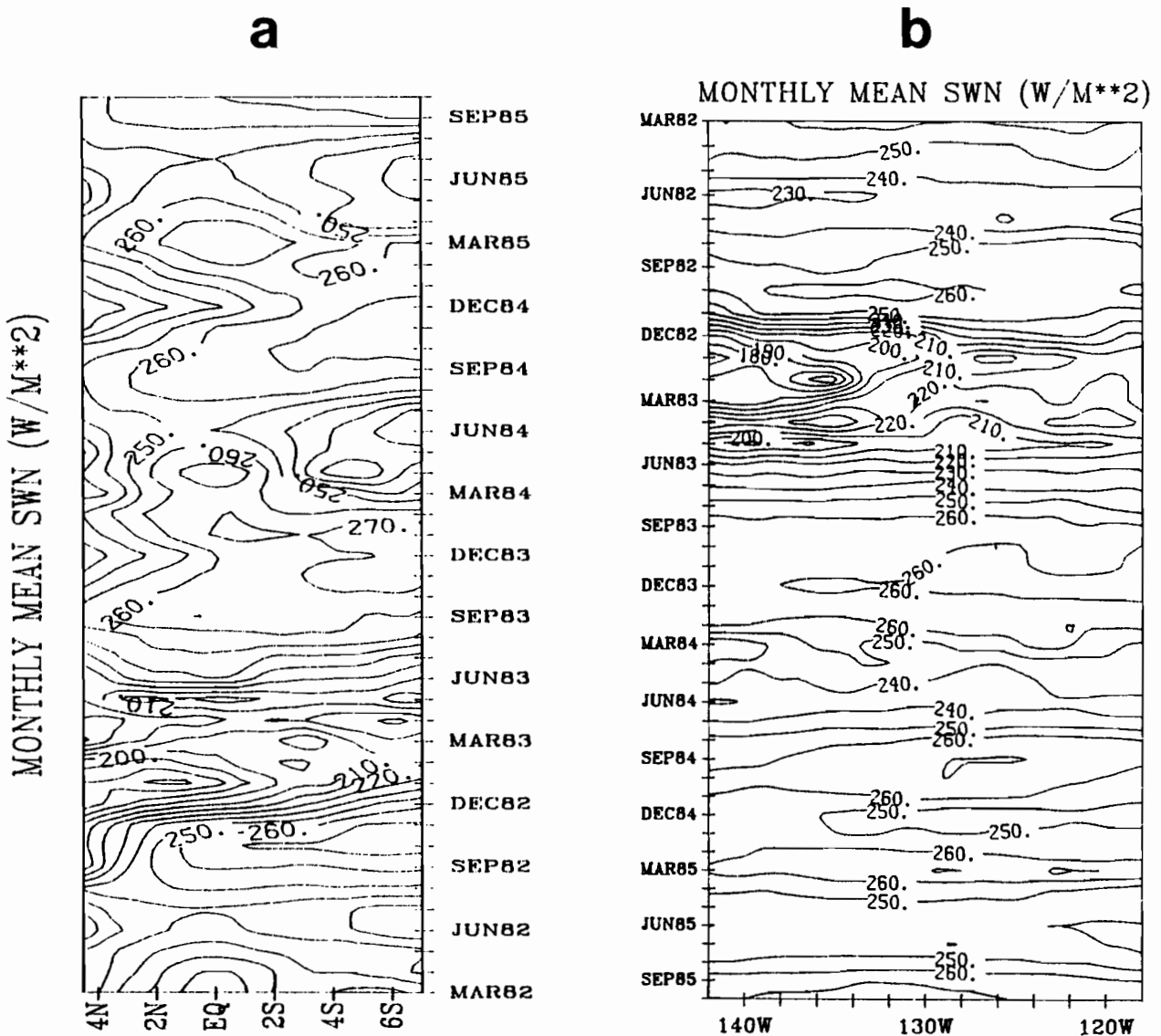


Fig. 3 Diagrams of time vs latitude (a) and time vs longitude (b)

The spatial and temporal variability of the net solar irradiance fields can be further quantified using empirical orthogonal function (EOF) analysis. An EOF analysis has been applied to two types of fields including and excluding the seasonal cycle: (1) difference fields from an annual mean (October 1984 to September 1985) and (2) difference fields from the monthly mean for each month of that same year. The annual mean removed from the first data set is shown in Fig. 4a and the square root of the variance (standard deviation) analyzed is illustrated Fig. 4b. The standard deviation field exhibits values ranging from $15 Wm^{-2}$ to $32 Wm^{-2}$ and a very high spatial variability (no direction is privileged).

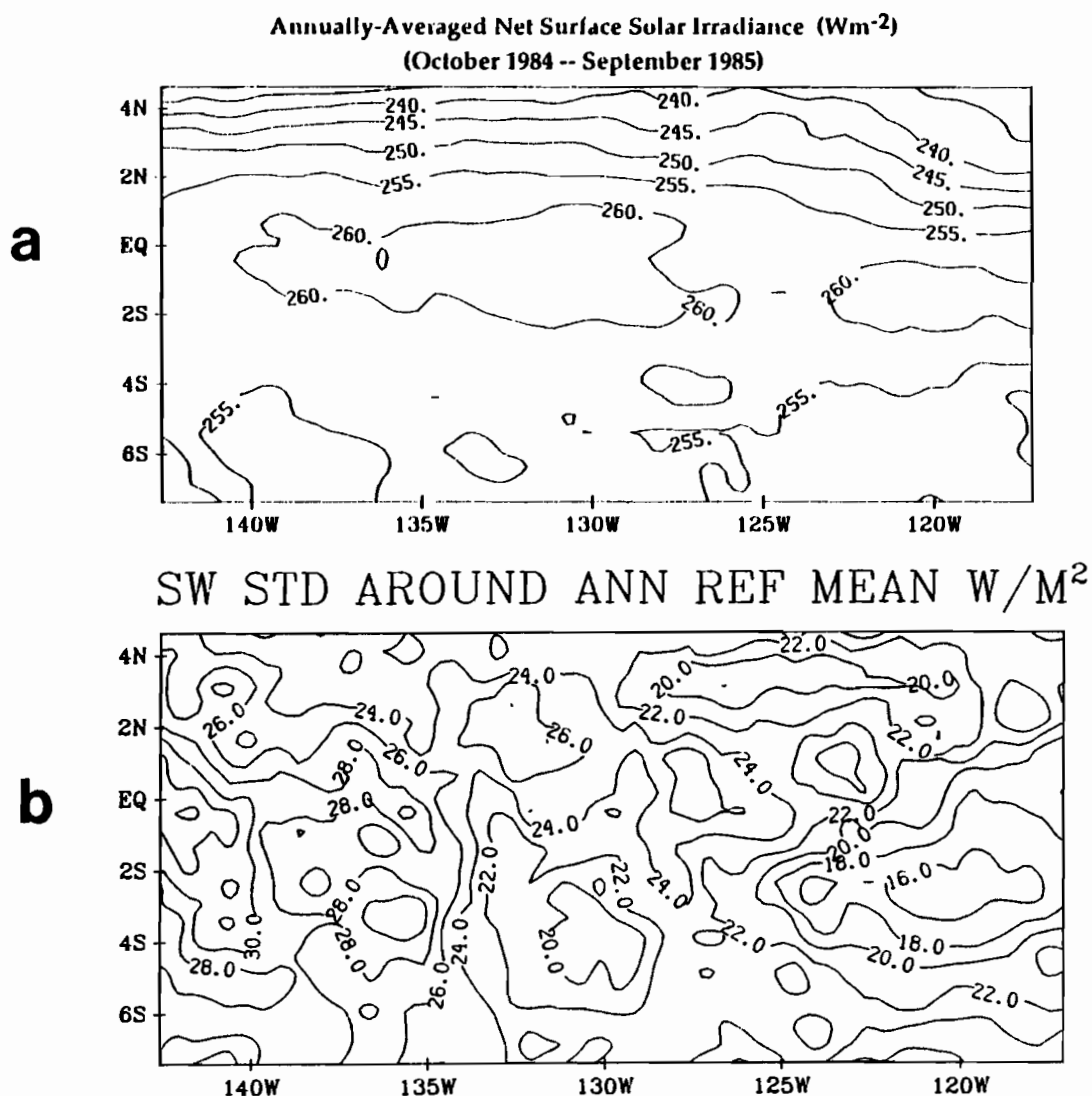
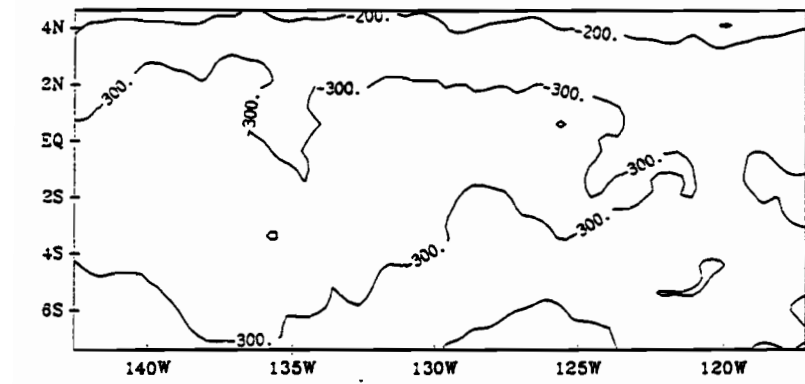
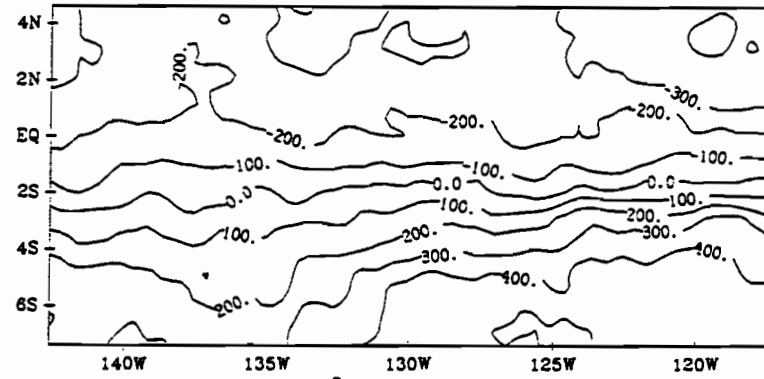


Fig. 4 Annually averaged net surface solar irradiance used for computing the anomalies (a) and the standard deviation around this mean of data used in the EOF analysis (b).

The EOF analysis of the first data set provides us with mostly the seasonal signals: semi-annual and annual. The first two EOFs explain 62.2 and 16.1 % of the variance (78.3 % cumulative), respectively, whereas the two subsequent EOFs each explain less than 5 % of the variance. The remaining EOFs each account for less than 2% of the variance. The first eigenfunction is presented together with its corresponding time varying amplitude coefficient in Fig. 5a. The values of this eigenfunction are small (3×10^{-2}) and negative everywhere; the spatial variability is small and a weak maximum exists in the equatorial region, centered around 2.5° S. The time variability of the amplitude coefficient is dominated by a semi-annual signal (cf. clear net surface solar irradiance plotted on the same graph with scaled amplitude). The semi-annual cycle is strongly perturbed by the El Niño event. The secondary maximum of December is strongly enhanced and delayed by a month whereas the primary maximum of June occurs earlier, after a much reduced minimum. These effects obviously result from cloud variations which counteract the normal sun variation effects and perturb the



a



b

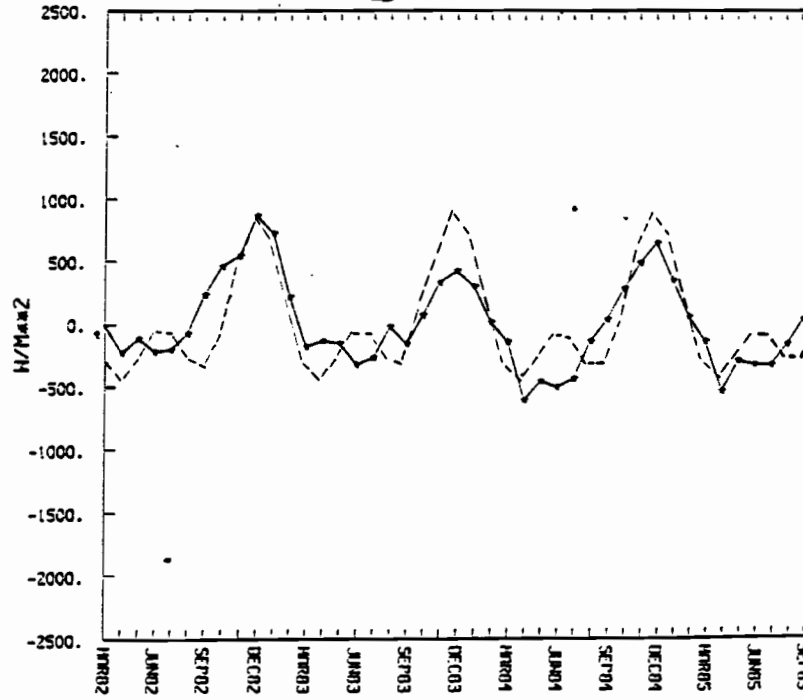
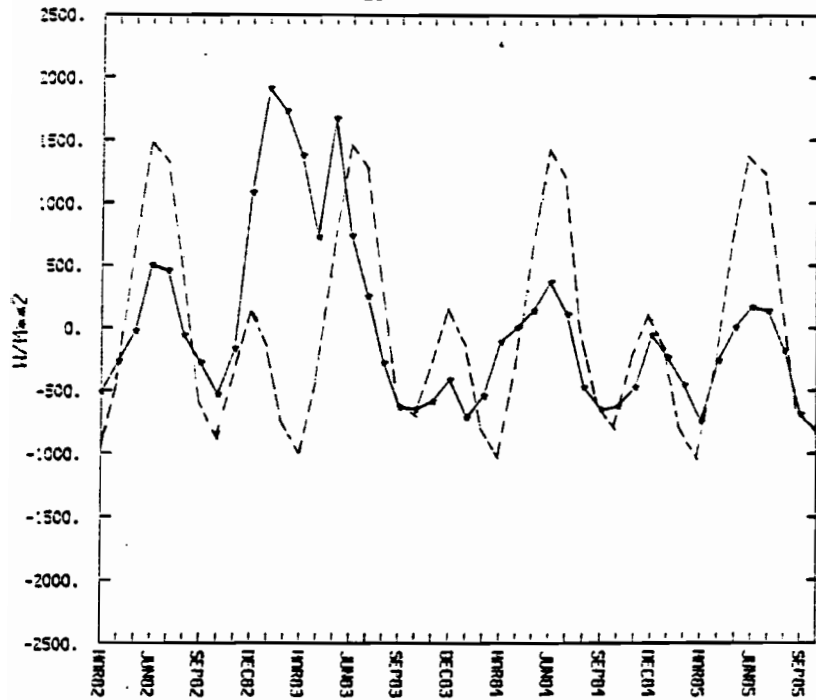


Fig. 5. The first (a) and second (b) empirical orthogonal functions (EOFs) of the seasonal data set. The top figures represent the eigenfunctions, and the bottom figures depict the time variations of associated amplitude coefficient (continuous line) and equivalent coefficient for clear-sky conditions (dashed line).

semi-annual cycle. The amplitude of the semi-annual signal for the area studied is about 30 Wm^{-2} during the years preceding and following El Niño.

The second eigenfunction and its corresponding time varying coefficient are presented in Fig 5b. The function field is very zonal and composed of negative values north of about 2.5° S and positive values south of 2.5° S . Because of the non-symmetry of the studied area, the zero isoline is located at about 2.5° S , instead of the equator, where it should be since this function represents the annual variations of the field. The amplitude coefficient has a strong annual signal with a marked maximum in November–December and a flat minimum around April–July, indicating that the north-south gradient changes sign annually. The El Niño appears to only slightly modify the annual signal (plotted on the same graph) by broadening the period of minimum from March to September 1983 and reducing the maximum. The amplitude of this annual signal varies with latitude; at about 5° S , it is about 30 Wm^{-2} and very similar to the semi-annual signal.

The first EOF of the non-seasonal data set is presented in Fig. 6a. It represents 67% of the total variance, while all the remaining EOFs represent less than 5 %. The spatial variability of the field is very similar to that of the first eigenfunction of the seasonal data set, with the largest value of the coefficients in the western equatorial region. The corresponding amplitude is presented in Fig 6b. It clearly shows the El Niño effect from December 1982 to June 1983. The maximum variation of net solar irradiance during that period was about -75 Wm^{-2} for about 3 months and less than -50 Wm^{-2} for another three months in the western equatorial region. An important aspect to note is the negative values of the amplitude coefficient (corresponding to 10 to 40 Wm^{-2} depending on the region) for most of the time after June 1983, suggesting anomalously clear sky conditions. These conditions were indeed noticed in our analysis of the anomaly fields not presented here.

The results presented above clearly indicate the strong effect the 1982-83 El Niño had on the net solar irradiance of the central equatorial Pacific. The western part of the area studied was in an anomalous state from September 1982 to August 1983. The reduction of net solar irradiance was more than 50 Wm^{-2} for several months. Such a large reduction of net solar irradiance over such a long time period suggests a possible feedback mechanism on the anomalously warm sea surface temperature then existing in the central equatorial Pacific. Whereas the warm sea surface temperature appears to precede the reduction of net solar irradiance, it can be expected that the lasting low values of net solar irradiance might induce a reduction of the warm anomaly during the subsequent months.

A study of the entire tropical Pacific solar irradiance has been recently initiated using data from two geostationary satellites to cover the entire width of the basin. The GMS satellite data have been used to complement the GOES data and compute solar irradiance in the eastern Pacific. The region of the warm pool is found to be dominated by deep convection of a similar nature to that observed in the central Pacific during El Niño.

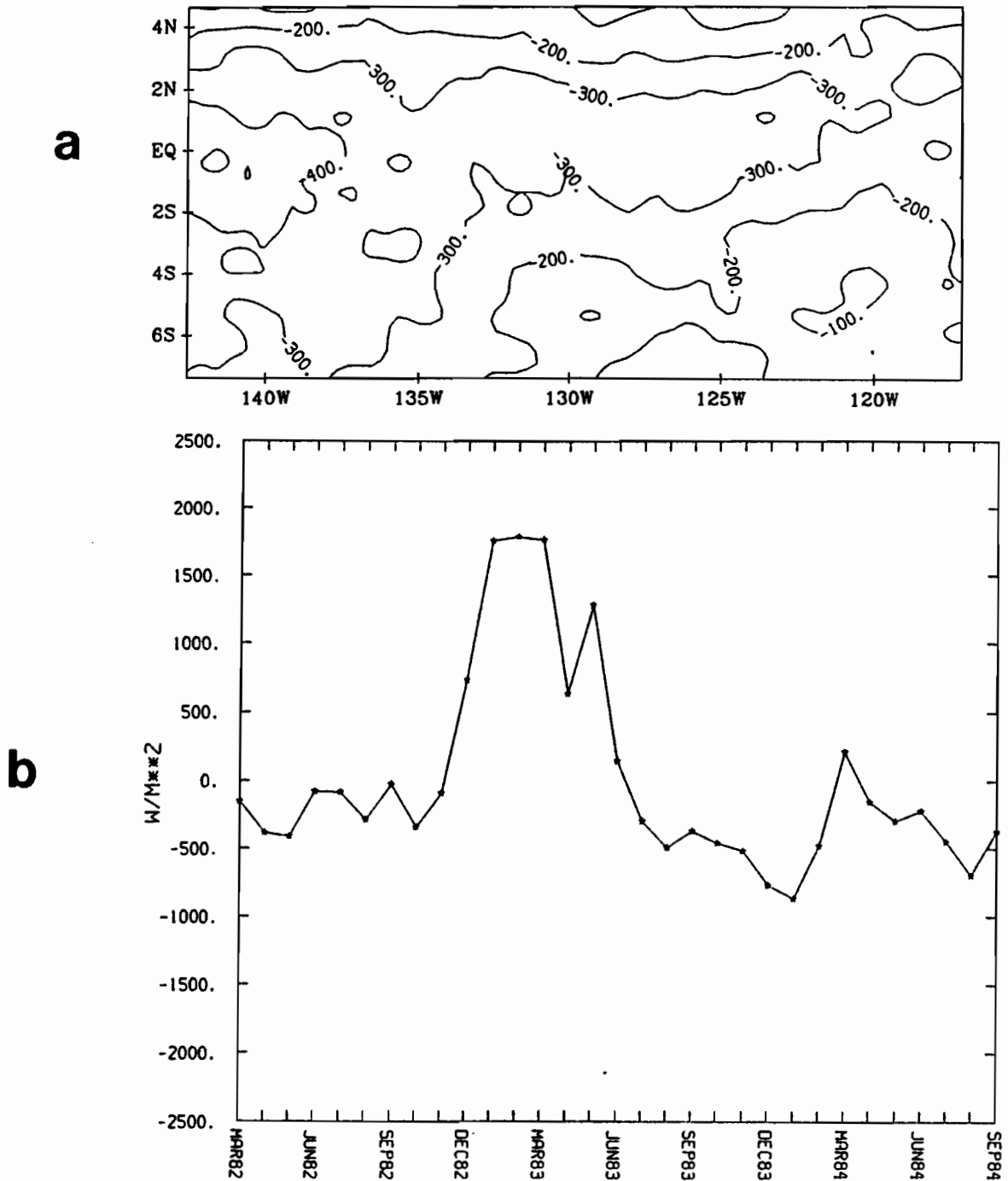


Fig. 6 First empirical orthogonal function of the non-seasonal data set (a) and time variations of associated amplitude coefficient (b).

Acknowledgments

This work has been supported by the National Oceanic and Atmospheric Administration's TOGA Project Office (NA86AA-DAC051) and through a research grant from the National Science Foundation (OCE-8717654). We are grateful for the technical support provided by Mr. Bob Wylie, Ms. Beth DiGiulio, and Mr. Brian Bloomfield.

References

- Budyko, M. L., 1963: Atlas of the Heat Balance of the Earth, (in Russian). Kartfabrika Gosgeoltekhizdata, Leningrad.
- Chou, M. D., 1985: Surface radiation in the tropical Pacific. *J. of Clim. and Appl. Meteorol.*, **24**, 83–92.
- Esbensen, S. K., and Y. Kushnir, 1981: The heat budget of the global oceans: An atlas based on surface marine observations. Rep. 29, Clim. Res. Inst., Oreg. State Univ., Corvallis.
- Gautier, C., G. Diak, and S. Masse, 1980: A simple physical model to estimate incident solar radiation at the surface from GOES satellite data. *J. Appl. Meteorol.*, **19**, 1005–1012.
- Gautier, C., and R. Frouin, 1989: Net surface solar irradiance variability in the central tropical Pacific. (In preparation).
- Weare, B. C., P.T. Strub, and M. D. Samuel, 1981: Annual mean surface heat fluxes in the tropical Pacific Ocean. *J. Phys. Oceanogr.*, **11**, 705–717.
- Wyrtki, K, 1965: The average annual heat balance of the North Pacific Ocean and its relation to ocean circulation. *J. Geophys. Res.*, **70**, 4547–4559.

**WESTERN PACIFIC INTERNATIONAL MEETING
AND WORKSHOP ON TOGA COARE**

Nouméa, New Caledonia

May 24-30, 1989

PROCEEDINGS

edited by

Joël Picaut *

Roger Lukas **

Thierry Delcroix *

* ORSTOM, Nouméa, New Caledonia

** JIMAR, University of Hawaii, U.S.A.

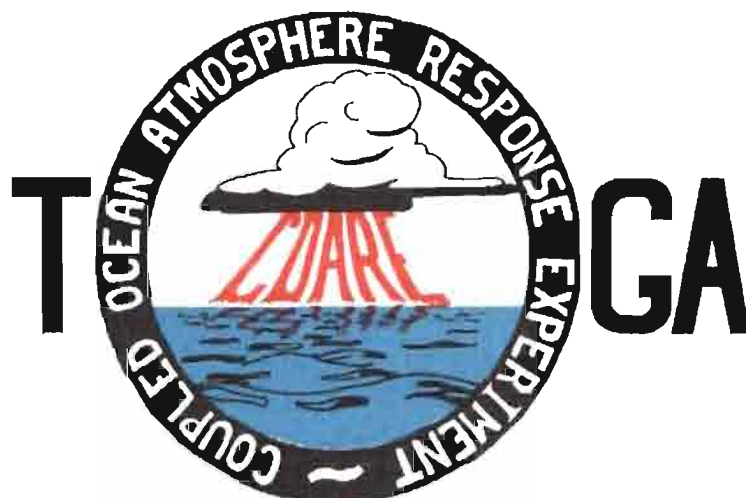


TABLE OF CONTENTS

ABSTRACT	i
RESUME	iii
ACKNOWLEDGMENTS	vi
INTRODUCTION	
1. Motivation	1
2. Structure	2
LIST OF PARTICIPANTS	5
AGENDA	7
WORKSHOP REPORT	
1. Introduction	19
2. Working group discussions, recommendations, and plans	20
a. Air-Sea Fluxes and Boundary Layer Processes	20
b. Regional Scale Atmospheric Circulation and Waves	24
c. Regional Scale Oceanic Circulation and Waves	30
3. Related programs	35
a. NASA Ocean Processes and Satellite Missions	35
b. Tropical Rainfall Measuring Mission	37
c. Typhoon Motion Program	39
d. World Ocean Circulation Experiment	39
4. Presentations on related technology	40
5. National reports	40
6. Meeting of the International Ad Hoc Committee on TOGA COARE	40
APPENDIX: WORKSHOP RELATED PAPERS	
Robert A. Weller and David S. Hosom: Improved Meteorological Measurements from Buoys and Ships for the World Ocean Circulation Experiment	45
Peter H. Hildebrand: Flux Measurement using Aircraft and Radars	57
Walter F. Dabberdt, Hale Cole, K. Gage, W. Ecklund and W.L. Smith: Determination of Boundary-Layer Fluxes with an Integrated Sounding System	81

MEETING COLLECTED PAPERS

WATER MASSES, SEA SURFACE TOPOGRAPHY, AND CIRCULATION

Klaus Wyrtki: Some Thoughts about the West Pacific Warm Pool	99
Jean René Donguy, Gary Meyers, and Eric Lindstrom: Comparison of the Results of two West Pacific Oceanographic Expeditions FOC (1971) and WEPOCS (1985-86)	111
Dunxin Hu, and Maochang Cui: The Western Boundary Current in the Far Western Pacific Ocean	123
Peter Hacker, Eric Firing, Roger Lukas, Philipp L. Richardson, and Curtis A. Collins: Observations of the Low-latitude Western Boundary Circulation in the Pacific during WEPOCS III	135
Stephen P. Murray, John Kindle, Dharma Arief, and Harley Hurlburt: Comparison of Observations and Numerical Model Results in the Indonesian Throughflow Region	145
Christian Henin: Thermohaline Structure Variability along 165°E in the Western Tropical Pacific Ocean (January 1984 - January 1989)	155
David J. Webb, and Brian A. King: Preliminary Results from Charles Darwin Cruise 34A in the Western Equatorial Pacific	165
Warren B. White, Nicholas Graham, and Chang-Kou Tai: Reflection of Annual Rossby Waves at The Maritime Western Boundary of the Tropical Pacific	173
William S. Kessler: Observations of Long Rossby Waves in the Northern Tropical Pacific	185
Eric Firing, and Jiang Songnian: Variable Currents in the Western Pacific Measured During the US/PRC Bilateral Air-Sea Interaction Program and WEPOCS	205
John S. Godfrey, and A. Weaver: Why are there Such Strong Steric Height Gradients off Western Australia ?	215
John M. Toole, R.C. Millard, Z. Wang, and S. Pu: Observations of the Pacific North Equatorial Current Bifurcation at the Philippine Coast	223

EL NINO/SOUTHERN OSCILLATION 1986-87

Gary Meyers, Rick Bailey, Eric Lindstrom, and Helen Phillips: Air/Sea Interaction in the Western Tropical Pacific Ocean during 1982/83 and 1986/87	229
Laury Miller, and Robert Cheney: GEOSAT Observations of Sea Level in the Tropical Pacific and Indian Oceans during the 1986-87 El Nino Event	247
Thierry Delcroix, Gérard Eldin, and Joël Picaut: GEOSAT Sea Level Anomalies in the Western Equatorial Pacific during the 1986-87 El Nino, Elucidated as Equatorial Kelvin and Rossby Waves	259
Gérard Eldin, and Thierry Delcroix: Vertical Thermal Structure Variability along 165°E during the 1986-87 ENSO Event	269
Michael J. McPhaden: On the Relationship between Winds and Upper Ocean Temperature Variability in the Western Equatorial Pacific	283

John S. Godfrey, K. Ridgway, Gary Meyers, and Rick Bailey: Sea Level and Thermal Response to the 1986-87 ENSO Event in the Far Western Pacific	291
Joël Picaut, Bruno Camusat, Thierry Delcroix, Michael J. McPhaden, and Antonio J. Busalacchi: Surface Equatorial Flow Anomalies in the Pacific Ocean during the 1986-87 ENSO using GEOSAT Altimeter Data	301

THEORETICAL AND MODELING STUDIES OF ENSO AND RELATED PROCESSES

Julian P. McCreary, Jr.: An Overview of Coupled Ocean-Atmosphere Models of El Nino and the Southern Oscillation	313
Kensuke Takeuchi: On Warm Rossby Waves and their Relations to ENSO Events	329
Yves du Penhoat, and Mark A. Cane: Effect of Low Latitude Western Boundary Gaps on the Reflection of Equatorial Motions	335
Harley Hurlburt, John Kindle, E. Joseph Metzger, and Alan Wallcraft: Results from a Global Ocean Model in the Western Tropical Pacific	343
John C. Kindle, Harley E. Hurlburt, and E. Joseph Metzger: On the Seasonal and Interannual Variability of the Pacific to Indian Ocean Throughflow	355
Antonio J. Busalacchi, Michael J. McPhaden, Joël Picaut, and Scott Springer: Uncertainties in Tropical Pacific Ocean Simulations: The Seasonal and Interannual Sea Level Response to Three Analyses of the Surface Wind Field	367
Stephen E. Zebiak: Intraseasonal Variability - A Critical Component of ENSO ?	379
Akimasa Sumi: Behavior of Convective Activity over the "Jovian-type" Aqua-Planet Experiments	389
Ka-Ming Lau: Dynamics of Multi-Scale Interactions Relevant to ENSO	397
Pecheng C. Chu and Roland W. Garwood, Jr.: Hydrological Effects on the Air-Ocean Coupled System	407
Sam F. Jacobellis, and Richard C.J. Somerville: A one Dimensional Coupled Air-Sea Model for Diagnostic Studies during TOGA-COARE	419
Allan J. Clarke: On the Reflection and Transmission of Low Frequency Energy at the Irregular Western Pacific Ocean Boundary - a Preliminary Report	423
Roland W. Garwood, Jr., Pecheng C. Chu, Peter Muller, and Niklas Schneider: Equatorial Entrainment Zone : the Diurnal Cycle	435
Peter R. Gent: A New Ocean GCM for Tropical Ocean and ENSO Studies	445
Wasito Hadi, and Nuraini: The Steady State Response of Indonesian Sea to a Steady Wind Field	451
Pedro Ripa: Instability Conditions and Energetics in the Equatorial Pacific	457
Lewis M. Rothstein: Mixed Layer Modelling in the Western Equatorial Pacific Ocean	465
Neville R. Smith: An Oceanic Subsurface Thermal Analysis Scheme with Objective Quality Control	475
Duane E. Stevens, Qi Hu, Graeme Stephens, and David Randall: The hydrological Cycle of the Intraseasonal Oscillation	485
Peter J. Webster, Hai-Ru Chang, and Chidong Zhang: Transmission Characteristics of the Dynamic Response to Episodic Forcing in the Warm Pool Regions of the Tropical Oceans	493

MOMENTUM, HEAT, AND MOISTURE FLUXES BETWEEN ATMOSPHERE AND OCEAN

W. Timothy Liu: An Overview of Bulk Parametrization and Remote Sensing of Latent Heat Flux in the Tropical Ocean	513
E. Frank Bradley, Peter A. Coppin, and John S. Godfrey: Measurements of Heat and Moisture Fluxes from the Western Tropical Pacific Ocean	523
Richard W. Reynolds, and Ants Leetmaa: Evaluation of NMC's Operational Surface Fluxes in the Tropical Pacific	535
Stanley P. Hayes, Michael J. McPhaden, John M. Wallace, and Joël Picaut: The Influence of Sea-Surface Temperature on Surface Wind in the Equatorial Pacific Ocean	543
T.D. Keenan, and Richard E. Carbone: A Preliminary Morphology of Precipitation Systems In Tropical Northern Australia	549
Phillip A. Arkin: Estimation of Large-Scale Oceanic Rainfall for TOGA	561
Catherine Gautier, and Robert Frouin: Surface Radiation Processes in the Tropical Pacific	571
Thierry Delcroix, and Christian Henin: Mechanisms of Subsurface Thermal Structure and Sea Surface Thermo-Haline Variabilities in the South Western Tropical Pacific during 1979-85 - A Preliminary Report	581
Greg. J. Holland, T.D. Keenan, and M.J. Manton: Observations from the Maritime Continent : Darwin, Australia	591
Roger Lukas: Observations of Air-Sea Interactions in the Western Pacific Warm Pool during WEPOCS	599
M. Nunez, and K. Michael: Satellite Derivation of Ocean-Atmosphere Heat Fluxes in a Tropical Environment	611

EMPIRICAL STUDIES OF ENSO AND SHORT-TERM CLIMATE VARIABILITY

Klaus M. Weickmann: Convection and Circulation Anomalies over the Oceanic Warm Pool during 1981-1982	623
Claire Perigaud: Instability Waves in the Tropical Pacific Observed with GEOSAT	637
Ryuichi Kawamura: Intraseasonal and Interannual Modes of Atmosphere-Ocean System Over the Tropical Western Pacific	649
David Gutzler, and Tamara M. Wood: Observed Structure of Convective Anomalies	659
Siri Jodha Khalsa: Remote Sensing of Atmospheric Thermodynamics in the Tropics	665
Bingrong Xu: Some Features of the Western Tropical Pacific: Surface Wind Field and its Influence on the Upper Ocean Thermal Structure	677
Bret A. Mullan: Influence of Southern Oscillation on New Zealand Weather	687
Kenneth S. Gage, Ben Basley, Warner Ecklund, D.A. Carter, and John R. McAfee: Wind Profiler Related Research in the Tropical Pacific	699
John Joseph Bates: Signature of a West Wind Convective Event in SSM/I Data	711
David S. Gutzler: Seasonal and Interannual Variability of the Madden-Julian Oscillation	723
Marie-Hélène Radenac: Fine Structure Variability in the Equatorial Western Pacific Ocean	735
George C. Reid, Kenneth S. Gage, and John R. McAfee: The Climatology of the Western Tropical Pacific: Analysis of the Radiosonde Data Base	741

Chung-Hsiung Sui, and Ka-Ming Lau: Multi-Scale Processes in the Equatorial Western Pacific	747
Stephen E. Zebiak: Diagnostic Studies of Pacific Surface Winds	757

MISCELLANEOUS

Rick J. Bailey, Helene E. Phillips, and Gary Meyers: Relevance to TOGA of Systematic XBT Errors	775
Jean Blanchot, Robert Le Borgne, Aubert Le Bouteiller, and Martine Rodier: ENSO Events and Consequences on Nutrient, Planktonic Biomass, and Production in the Western Tropical Pacific Ocean	785
Yves Dandonneau: Abnormal Bloom of Phytoplankton around 10°N in the Western Pacific during the 1982-83 ENSO	791
Cécile Dupouy: Sea Surface Chlorophyll Concentration in the South Western Tropical Pacific, as seen from NIMBUS Coastal Zone Color Scanner from 1979 to 1984 (New Caledonia and Vanuatu)	803
Michael Szabados, and Darren Wright: Field Evaluation of Real-Time XBT Systems	811
Pierre Rual: For a Better XBT Bathy-Message: Onboard Quality Control, plus a New Data Reduction Method	823